Journal of Solid State Chemistry **144,** 409–415 (1999)
Article ID jssc.1999.8188, available online at http://www.idealibrary.com on IDEAL®

Synthesis and Structure of a New Ternary Silver-Rich Sulfide $BaAg_8S_5$

Catherine E. Check,* Chong Zheng,*,[1] Jianhua Zhang,* Bogdan Dabrowski†

*Department of Chemistry and †Department of Physics, Northern Illinois University, DeKalb, Illinois 60115

Received May 26, 1998; in revised form January 26, 1999; accepted February 2, 1999

A new ternary silver-rich sulfide, $BaAg_8S_5$, was synthesized. This solid-state compound crystallizes in the monoclinic, centrosymmetric space group $P2_1/m$ with $a = 7.6720(2)$ Å, $b = 17.6660(4)$ Å, $c = 8.9370(2)$ Å, $\beta = 107.890(1)^\circ$, $Z = 4$, and $V = 1152.70(5)$ Å^3. The refinement results are $R1 = 0.0490$ and $wR2 = 0.1136$ for $I > 2\sigma(I)$ using 2552 reflections and 137 parameters. As in the binary α-Ag_2S and β-Ag_2S solids, the coordination geometry of both Ag and S is complex. However, if only the bonding of Ag to S is concerned, the arrangement is simple. Ag of the first type is connected to two S atoms in both linear and bent fashions. Ag of the second type is coordinated to three S atoms in a pyramidal shape. The structure can be viewed as a three-dimensional network formed by Ag and S atoms with Ba atoms occupying channels parallel to the *c* axis. Theoretical analysis using the extended Hückel method indicates that the solid should be a semiconductor.

INTRODUCTION

Silver chalcogenide solid state compounds have attracted renewed attention because of their magnetoresistant property at low and room temperatures (1). Binary silver sulfide, Ag_2S, which has several allotropic forms, is a fast-ion conductor above 177°C (2). Beyond the binary phase, several quaternary phases containing Ba, Ag, and S, such as $Ba_2LaAg_5S_6$, $BaErAgS_3$, and $BaSc_3AgS_6$ synthesized by Wu *et al.* (3–5) and Ag_2BaGeS_4 by Teske (6), have been reported. Not many ternary solid-state compounds of alkaline earth metal, silver and sulfur, however, have been described in the literature. One example, though, is $BaAg_2S_2$ synthesized by Bronger and his co-workers using a novel approach where barium-*bis*[dicyanoargentate(I)] is used as the starting material (7). In this article, we summarize the synthesis, structural determination, and computational study of another ternary compound $BaAg_8S_5$.

[1]To whom correspondence should be addressed. E-mail: zheng@cz2.chem.niu.edu.

EXPERIMENTAL

Synthesis

The compound $BaAg_8S_5$ was prepared by a standard solid-state synthesis. The reaction started from elemental Ag (Strem Chemicals, 99.9%) and S (Fisher Scientific, 99.5%) along with the binary sulfide BaS (Alfa, 99.7%) in the molar ratio of 2:1:1. The reactants were ground together and pressed into a pellet. The pellet was placed in a quartz ampoule, which was then evacuated to about 10^{-4} Torr and sealed. The quartz ampoule was placed in a computer-controlled furnace and heated from room temperature to 1100°C over a period of 12 h. This temperature was maintained for 72 h. The quartz ampoule was then cooled from 1100°C to room temperature over a period of 24 h. The reaction was repeated two more times to confirm the presence of the new phase. All three reactions resulted in black crystals of the title compound. In addition to the $BaAg_8S_5$ compound with a yield of less than 10%, binary barium sulfides BaS (8), BaS_2 (9), and BaS_3 (10) were also present in the product as revealed by subsequent powder as well as single crystal x-ray diffraction measurements. $BaAg_8S_5$ could also be synthesized by using the appropriate stoichiometric ratio of Ba, Ag, and S, or BaS and Ag_2S, with a better yield ($< 20\%$).

Crystallographic Study and Elemental Analysis

Several black crystals of the title compound were indexed on a Siemens SMART CCD diffractometer using 40 frames with an exposure time of 20 s per frame. All of them showed a monoclinic cell, and the systematic absence of $k = 2n + 1$ is consistent with the space group $P2_1/m$. One crystal with good reflection quality was chosen and mounted on an Enraf-Nonius CAD4 diffractometer. Twenty-five reflections were collected to index the unit cell. A total of 2711 reflections were collected with an orientation and intensity check of every 250 reflections using three standard reflections during the data collection. An empirical ψ-scan absorption correction was applied to all observed reflections (2562 unique reflections). The structure was solved with the direct

0022-4596/99 $30.00

method using both the SHELXS (11) and SIR92 (12) programs; both programs gave the same structure. Refinement on F^2 was carried out using the SHELXL-93 program (11). The final agreement factor values are $R1 = 0.0490$, w$R2 = 0.1136$ ($I > 2\sigma$). The final structure was checked for additional symmetry with the MISSYM algorithm (13) implemented in the PLATON program suite (14). No additional symmetry was found. The unit cell information and refinement details are reported in Table 1. The atomic positions and equivalent isotropic displacement parameters are listed in Table 2. Selected bond lengths and angles are in Table 3.

An EDAX analysis using the microprobe of a JEOL 35 CF-Kevex μx 7000 scanning electron microscope confirmed the presence of all three elements. The approximate ratio of the three elements in the same crystal used for the crystallographic study was determined to be Ba:Ag:S = 1.0:8.3:5.3.

RESULTS AND DISCUSSION

Structural Features

The structure is shown in Fig. 1. It is a three-dimensional network formed by Ag and S atoms with channels which Ba atoms occupy. It can also be viewed as stacking complex Ag–S layers (see Fig. 2) separated by Ba channels if the S atoms (S13, S15) connecting the layers are ignored. There are two Ba channels and two Ag–S layers per unit cell. The Ag–S layers are joined by the S atoms S13 and S15 in each cell. Each layer is connected to a layer above by these two S atoms and to a layer below by the inversion equivalents of these S atoms. The coordination geometry of these S atoms, S13 and S15, is shown in Fig. 3. The S15 atom connects two layers by forming two bonds (2.43 Å) to two Ag atoms in the layers above and below. The Ag–S–Ag bond angle is 76° (Notice that in Fig. 3 the Ag–S–Ag trimer is shown horizontally, but in Fig. 1 it is vertical and approximately parallel to the *b* axis; the same is true for the S atom S13). The S13 atom connects the layers through four S–Ag bonds. The bond lengths range from 2.44 to 2.66 Å. The smallest Ag–S–Ag angle at the S13 center is 81°. Because of the connection between the Ag–S layers, the Ba atoms form columns in the channels rather than sheets in the structure. The complexity of the Ag–S layer is shown in Fig. 2, where the Ba channels can be viewed down the *a* axis. It can be seen in this figure that the Ag coordination is not as regular as that in both the low-T and high-T phases of β-Ag_2S. In these binary phases, Ag coordination is mainly octahedral or tetrahedral (2). In $Ba_2LaAg_5S_6$, Ag coordination is either tetrahedral or linear (3).

The local geometry of various Ba, Ag, and S atoms in the compound is shown in Fig. 3. Coordination is more complicated around the S atoms. Some S atoms (S15) are bonded to only two Ag atoms, others to three (S14, S16, and S17), four (S13), or even five (S12) atoms. The bond lengths range from 2.42 to 2.66 Å, comparable to the sum of the

TABLE 1
Crystal Data and Structure Refinement for $BaAg_8S_5$

Empirical formula	Ag8 Ba S5
Formula weight	1160.60
Temperature	293(2) K
Wavelength	0.71073 Å
Crystal system	Monoclinic
Space group	$P2_1/m$
Unit cell dimensions	$a = 7.6720(2)$ Å $b = 17.6660(4)$ Å $\beta = 107.890(1)^\circ$ $c = 8.9370(2)$ Å
Volume, Z	1152.70(5) Å^3, 4
Density (calculated)	6.688 mg/m^3
Absorption coefficient	17.486 mm^{-1}
F(000)	2048
Crystal size	$0.06 \times 0.04 \times 0.04$ mm
Theta range for data collection	3.02 to 26.98°
Limiting indices	$-9 \le h \le 9$, $0 \le k \le 21$, $0 \le l \le 10$
Reflections collected	2711
Independent reflections	2562 [R(int) = 0.0426]
Absorption correction	Psi-scan
Maximum and minimum transmission	0.0594 and 0.0260
Refinement method	Full-matrix least-squares on F^2
Data / restraints / parameters	2552 / 0 / 137
Goodness-of-fit on F^2	1.124
Final R indices[a] [$I > 2\sigma(I)$]	$R1 = 0.0490$, w$R2 = 0.1136$
R indices (all data)	$R1 = 0.0654$, w$R2 = 0.1390$
Extinction coefficient	0.00034(11)

[a] $R1 = \sum||F_o| - |F_c||/\sum|F_o|$; w$R2 = [\sum[w(F_o^2 - F_c^2)^2]/\sum[w(F_o^2)^2]]^{1/2}$.

TABLE 2
Atomic Coordinates ($\times 10^4$) and Equivalent Isotropic Displacement Parameters (Å$^2 \times 10^3$) for $BaAg_8S_5$

	Site	x	y	z	U_{eq}
Ba(1)	2*e*	4041(2)	7500	7148(1)	23(1)
Ba(2)	2*e*	4466(2)	7500	2522(1)	23(1)
Ag(3)	4*f*	− 889(2)	6600(1)	4612(2)	42(1)
Ag(4)	2*a*	0	5000	10000	42(1)
Ag(5)	4*f*	8879(2)	6654(1)	7791(2)	45(1)
Ag(6)	4*f*	2634(2)	5967(1)	9296(1)	39(1)
Ag(7)	4*f*	− 446(2)	6634(1)	1318(2)	43(1)
Ag(8)	4*f*	6824(2)	5504(1)	2183(2)	53(1)
Ag(9)	4*f*	− 680(2)	5057(1)	6435(2)	46(1)
Ag(10)	4*f*	6265(2)	5540(1)	8384(2)	52(1)
Ag(11)	2*d*	5000	5000	5000	50(1)
S(12)	4*f*	2381(5)	5701(2)	2033(4)	25(1)
S(13)	2*e*	1063(6)	7500	3810(6)	23(1)
S(14)	4*f*	2262(5)	5703(2)	6442(4)	26(1)
S(15)	2*e*	1271(6)	7500	9317(6)	23(1)
S(16)	4*f*	6157(5)	6528(2)	10287(4)	25(1)
S(17)	4*f*	6348(5)	6356(2)	5421(4)	24(1)

Note. U_{eq} is defined as one third of the trace of the orthogonalized U_{ij} tensor.

TABLE 3
Selected Bond Lengths [Å] and Angles (deg) for $BaAg_8S_5$

Ba(1)-S(13)	3.152(5)	Ag(6)–S(14)	2.521(4)
Ba(1)–S(16) (×2)	3.265(4)	Ag(6)–S(12)#8	2.557(4)
Ba(1)–S(15)	3.288(5)	Ag(6)–S(16)	2.756(4)
Ba(1)–S(17) (×2)	3.358(4)	Ag(6)–S(15)	2.905(2)
Ba(1)–S(14) (×2)	3.436(4)	Ag(6)–Ag(8)#12	3.002(2)
Ba(1)–Ag(6) (×2)	3.668(2)	Ag(6)–Ag(5)#6	3.033(2)
Ba(1)–Ag(10) (×2)	3.868(2)	Ag(6)–Ag(10)	3.223(2)
Ba(2)–S(15)#2	3.146(5)	Ag(7)–S(16)#13	2.490(4)
Ba(2)–S(13)	3.160(5)	Ag(7)–S(12)	2.641(4)
Ba(2)–S(16)#2 (×2)	3.195(4)	Ag(7)–S(13)	2.657(4)
Ba(2)–S(17) (×2)	3.253(4)	Ag(7)–S(15)#2	2.953(4)
Ba(2)–S(12)#1	3.524(3)	Ag(7)–Ag(5)#13	3.033(2)
Ba(2)–Ag(3)#4 (×2)	3.825(2)	Ag(7)–Ag(7)#1	3.061(3)
Ba(2)–Ag(6)#2 (×2)	3.890(2)	Ag(7)–Ag(8)#6	3.156(2)
Ag(3)–S(13)	2.439(4)	Ag(8)–S(16)#2	2.423(4)
Ag(3)–S(17)#6	2.478(4)	Ag(8)–S(14)#12	2.454(4)
Ag(3)–Ag(5)#6	2.902(2)	Ag(8)–Ag(10)#12	2.922(2)
Ag(3)–S(14)	2.932(4)	Ag(8)–Ag(9)#12 (×2)	3.002(2)
Ag(3)–Ag(8)#6	3.032(2)	Ag(8)–Ag(3)#5	3.032(2)
Ag(3)–Ag(7)	3.067(2)	Ag(8)–Ag(7)#5	3.156(2)
Ag(3)–Ag(9)	3.154(2)		
Ag(3)–Ag(3)#1	3.181(3)	Ag(9)–S(14)	2.528(4)
		Ag(9)–S(12)#7	2.543(4)
Ag(4)–S(12)#7 (×2)	2.477(3)	Ag(9)–S(14)#7	2.823(4)
Ag(4)–Ag(6) (×2)	2.8605(13)	Ag(10)–Ag(8)#12	2.922(2)
Ag(4)–Ag(10)#6 (×2)	2.943(2)	Ag(9)–Ag(9)#7	3.058(3)
Ag(4)–Ag(9)#9 (×2)	3.068(2)	Ag(9)–Ag(5)#6	3.129(2)
Ag(4)–Ag(7)#8 (×2)	3.175(2)	Ag(9)–Ag(11)#6	3.1668(14)
		Ag(10)–S(16)	2.456(4)
		Ag(10)–S(12)#12	2.502(4)
Ag(5)–S(15)#5	2.434(4)	Ag(10)–Ag(8)#12	2.922(2)
Ag(5)–S(17)	2.451(4)	Ag(10)–Ag(4)#5	2.943(2)
Ag(5)–Ag(3)#5	2.902(2)	Ag(10)–Ag(11)	3.032(2)
Ag(5)–Ag(10)	2.971(2)		
Ag(5)–Ag(5)#1	2.991(3)	Ag(11)–S(17) (×2)	2.591(3)
Ag(5)–Ag(7)#11 (×2)	3.033(2)	Ag(11)–Ag(10)#12	3.032(2)
Ag(5)–Ag(9)#5	3.129(2)	Ag(11)–Ag(9)#7 (×2)	3.167(2)
S(13)–Ag(3)–S(17)#6	148.92(13)	S(13)–Ag(7)–S(15)#2	92.77(12)
S(13)–Ag(3)–Ag(5)#6	119.63(12)	S(12)–Ag(7)–S(15)#2	89.10(11)
S(17)#6–Ag(3)–S(14)	112.10(12)		
		S(16)#2–Ag(8)–S(14)#12	164.9(2)
S(12)#7–Ag(4)–S(12)#8	180.0		
		S(14)–Ag(9)–S(12)#7	147.36(13)
S(15)#5–Ag(5)–S(17)	151.24(14)	S(14)–Ag(9)–S(14)#7	110.55(10)
		S(12)#7–Ag(9)–S(14)#7	95.26(12)
S(14)–Ag(6)–S(12)#8	156.31(13)		
S(14)–Ag(6)–S(16)	100.78(12)	S(16)–Ag(10)–S(12)#12	146.07(14)
S(12)#8–Ag(6)–S(16)	96.52(12)		
S(14)–Ag(6)–S(15)	104.47(13)	S(17)–Ag(11)–S(17)#12	180.0
S(12)#8–Ag(6)–S(15)	91.82(13)		
S(16)–Ag(6)–S(15)	88.99(12)	Ag(4)#2–S(12)–Ag(10)#12	72.48(10)
		Ag(3)–S(13)–Ag(3)#1	81.4(2)
S(16)#13–Ag(7)–S(12)	136.98(13)	Ag(8)#12–S(14)–Ag(6)	74.21(11)
S(16)#13–Ag(7)–S(13)	119.35(14)	Ag(5)#6–S(15)–Ag(5)#14	75.8(2)
S(12)–Ag(7)–S(13)	92.43(12)	Ag(8)#8–S(16)–Ag(10)	84.77(13)
S(16)#13–Ag(7)–S(15)#2	115.21(13)	Ag(5)–S(17)–Ag(3)#5	72.13(10)

Note. Symmetry transformations used to generate equivalent atoms: #1 $x, -y+3/2, z$; #2 $x, y, z-1$; #3 $x, -y+3/2, z-1$; #4 $x+1, -y+3/2, z$; #5 $x+1, y, z$; #6 $x-1, y, z$; #7 $-x, -y+1, -z+1$; #8 $x, y, z+1$; #9 $-x, -y+1, -z+2$; #10 $-x+1, -y+1, -z+2$; #11 $x+1, y, z+1$; #12 $-x+1, -y+1, -z+1$; #13 $x-1, y, z-1$; #14 $x-1, -y+3/2, z$; #15 $x, -y+3/2, z+1$.

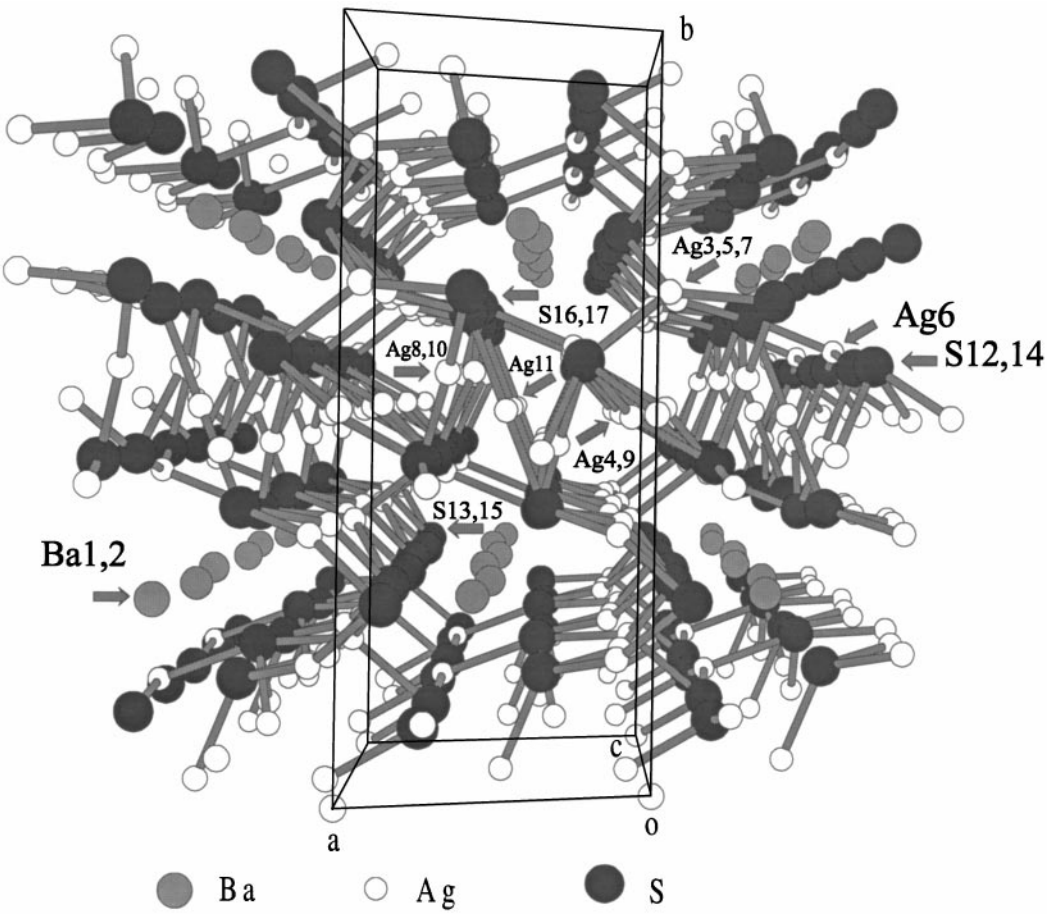

FIG. 1. The $BaAg_8S_5$ structure viewed down the *c* axis. The large shaded circles are Ba, the medium white circles are Ag, and the small black circles are S.

covalent radii of Ag (1.44 Å) and S (1.04 Å). If the Ag–Ag bonds are ignored, then the coordination around an Ag atom is simple. In the first type of coordination, each Ag atom is bonded to two S atoms, the coordination can be linear, as around Ag4 (and Ag11), or bent as around other Ag atoms (Ag3, 5, 7, 8, 10, 11) with bond angles from 149° to 156° (see Table 3). The geometry around Ag3 in Fig. 3 exemplifies such a bent trimer. The second type coordination involves three sulfur atoms around Ag6 and Ag9 in a pyramidal shape. If the contact beyond 3.0 Å is included, then the coordination around Ag6 and Ag7 can be traced to a distorted tetrahedron.

In this compound, there are several Ag–Ag contacts, ranging from 2.90 to 3.18 Å (see Table 3) that are slightly longer than the sum of the covalent radii of two Ag atoms (2.88 Å). It is probably due to the weak d^{10}–d^{10} interactions (15).

Computational Analysis

A formal electron partitioning of $Ba^{2+}(Ag^{+})_8(S^{2-})_5$ implies that the compound is in a closed-shell electronic configuration and thus a semiconductor. However, since the shortest Ag–Ag distance is around 2.90 Å, there is a possibility that the interaction among the Ag atoms may alter the conducting property of the compound. To understand the electronic structure of the title compound, we have carried out a computational study.

The band structure, density of states (DOS), and crystal orbital overlap population (COOP) were calculated using the extended Hückel tight-binding method (16–18). A set of 54 *k* points in the irreducible wedge of the Brillouin zone was used. The extended Hückel parameters are listed in Table 4.

The calculated DOS is shown in Fig. 4. At the extended Hückel level of computation, the compound is predicted indeed to be a semiconductor with a band gap of about 4.4 eV. As is well known, the extended Hückel method usually overestimates the magnitude of a band gap. The DOS around the Fermi level is mostly of Ag character. Below the Ag *d* states are two peaks of mostly *p* and *s* states of the sulfur atoms. Above the band gap, the states are nearly all Ag *s* and *p* states.

Figure 5 shows the computed average crystal orbital overlap population (COOP) curves (17) for the Ag–Ag and

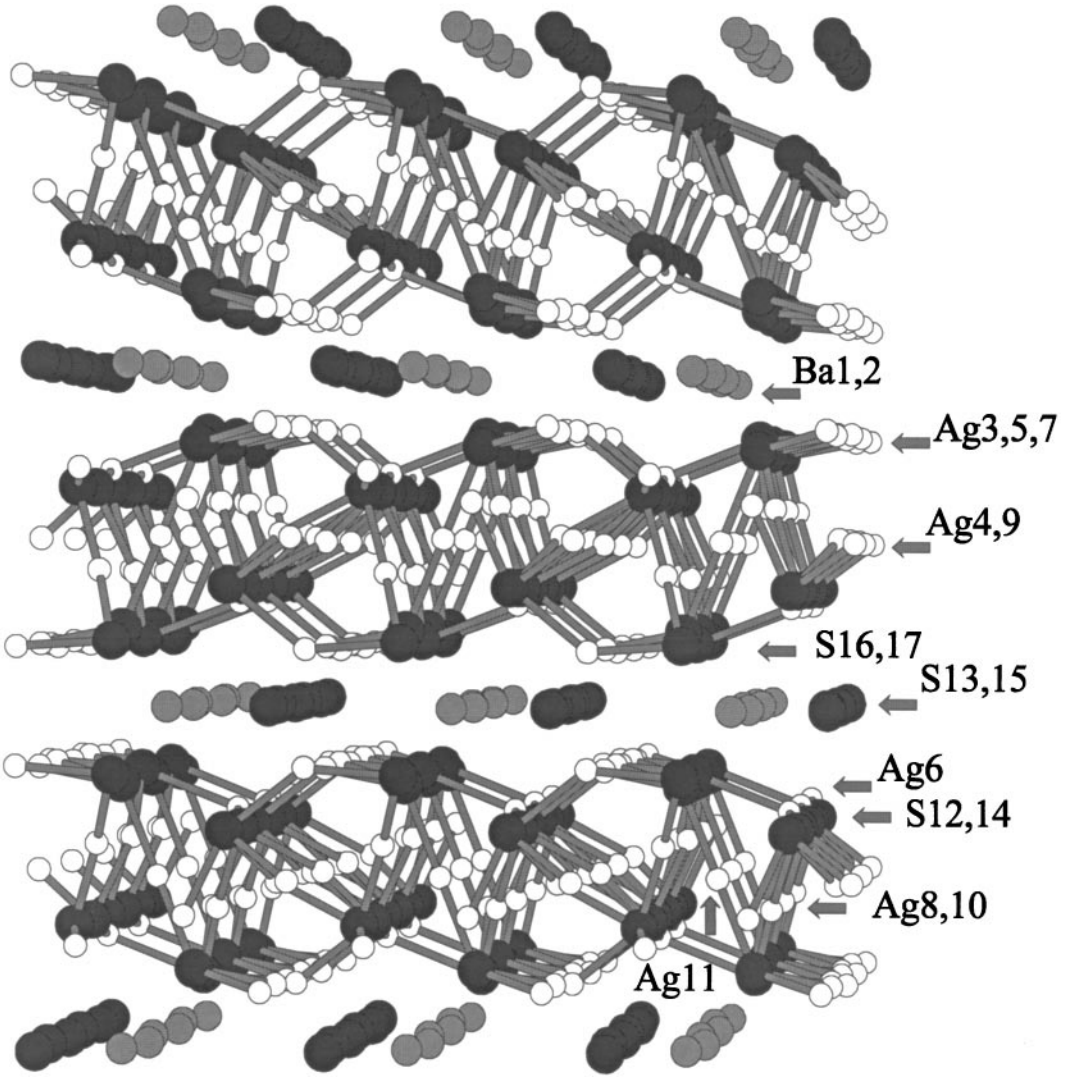

FIG. 2. A view along the *c* axis in the $BaAg_8S_5$ structure. The sulfur atoms S13, S15 join the layers. For clarity, the interlayer bonds connected to S13 and S15 are not plotted. The layers are parallel to the *a*–*c* plane.

TABLE 4
Extended Hückel Parameters (19–21)

	Orbital	H_{ii} (eV)	ζ_1[a]	ζ_2	c_1[a]	c_2
Ba	6*s*	− 7.0	1.2			
	6*p*	− 4.0	1.2			
Ag	5*s*	− 7.56	2.244			
	5*p*	− 3.83	2.244			
	4*d*	− 11.58	6.07	2.663	0.5889	0.6370
S	3*s*	− 20.0	1.817			
	3*p*	− 13.3	1.817			

[a]Exponents and coefficients in a double ζ expansion of the *d* orbital.

Ag–S bonds. The average is taken for all bonds in the unit cell. Both curves show some antibonding character for those states immediately below the Fermi level. For the Ag–Ag bond, the antibonding character is due to the filled *d* block. The lower part of the *d* block contributes to Ag–Ag bonding, the upper part to antibonding. The Ag–S antibonding character of the states just below the Fermi level is more difficult to understand because one would expect the states below the Fermi level contribute to Ag–S bonding. However, because of appreciable Ag–Ag interaction, some states which are of Ag–S antibonding and originally above the Fermi level are pulled down below the Fermi level by the Ag–Ag bonding interaction. Indeed, it was shown in our calculation that the amount of the Ag–S antibonding states

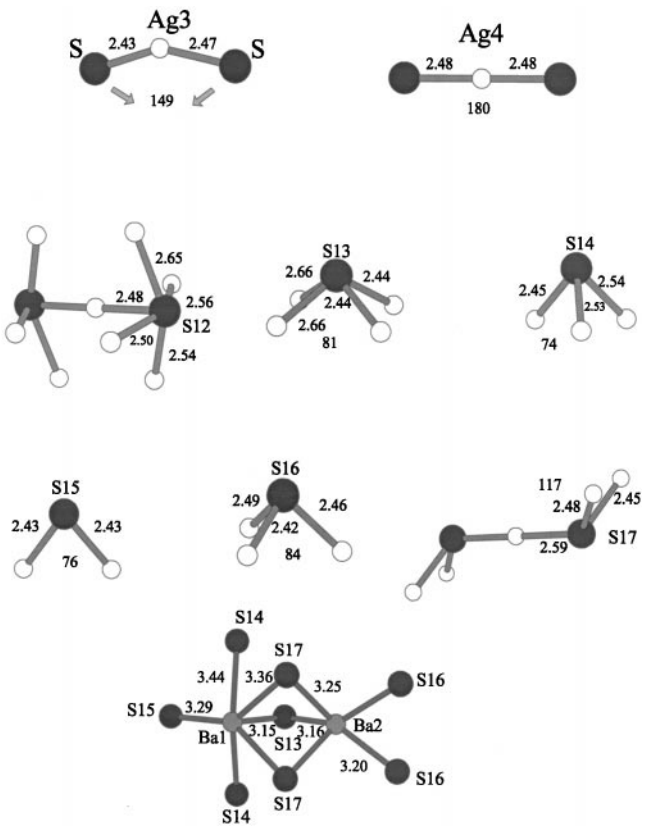

FIG. 3. Local coordination of the Ba, Ag, and S atoms.

decreases as the orbital overlap of the closest Ag–Ag contacts are deleted

As shown in Fig. 1, the structure of the title compound is pseudo two-dimensional. Therefore, we expect that the interaction is stronger within the layers than between them.

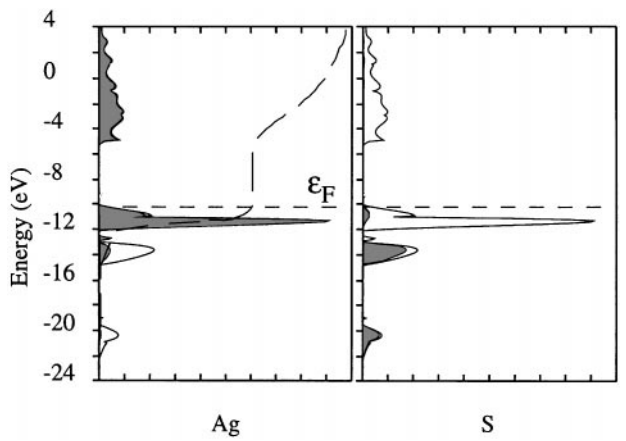

FIG. 4. The computed DOS of the $BaAg_8S_5$ structure. The solid line is the total DOS; the shaded area is the projected DOS of Ag (left) and S (right). The dashed line is the integrated projected DOS. The horizontal dashed line represents the Fermi level.

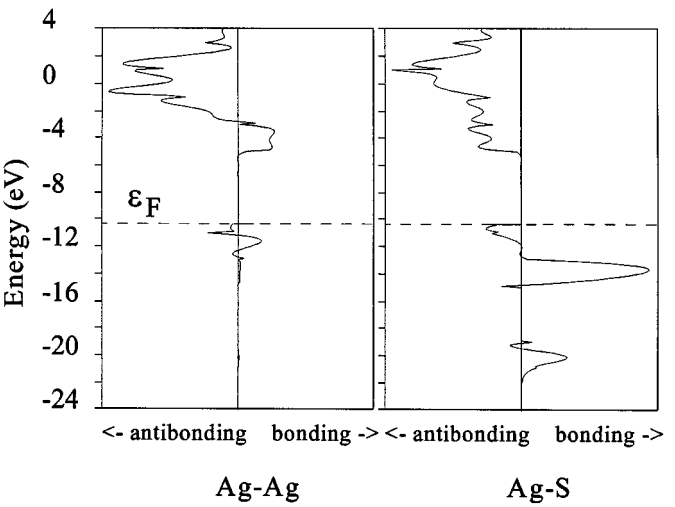

FIG. 5. The computed average COOP curves of the Ag–Ag and Ag–S bonds in the $BaAg_8S_5$ structure. The average is taken for all bonds in the unit cell.

This implies that the bands will have larger dispersion in the directions within the layer than in the direction perpendicular to it. Indeed, Fig. 6 shows the difference in the band dispersions in these two different directions. Because of the many atoms in the unit cell, the complete band structure is complicated. Only a portion near the region of -13 to -15 eV is shown. In this region, the states contribute mostly to Ag–S bonding, and thus the region is most important in the inter and intra layer interaction. In Fig. 6, the direction Y to Γ is perpendicular to the layers ([0, 0.5, 0]

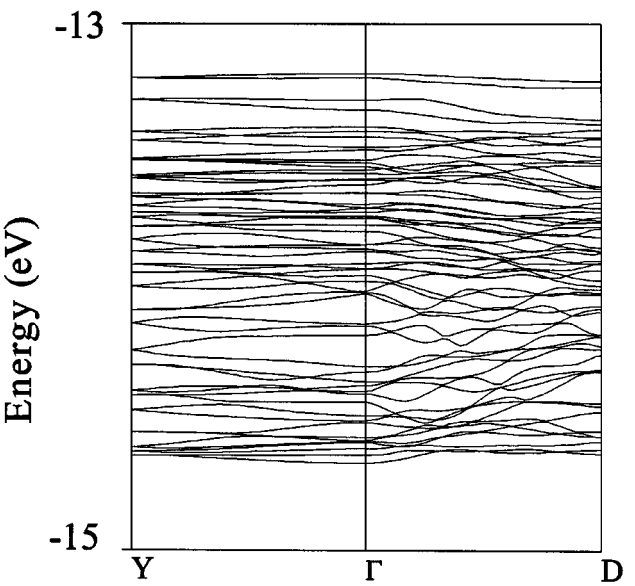

FIG. 6. The computed band structure in the region of -13 to -15 eV. The three special k points for the monoclinic lattice are Y [0, 0.5, 0], Γ [0, 0, 0], D [0.5, 0, 0.5].

to [0, 0, 0] in the reciprocal lattice), or parallel to the *b* axis, while the direction from Γ to *D* is parallel to the layer ([0, 0, 0] to [0.5, 0, 0.5] in the reciprocal lattice).

CONCLUSION

The silver-rich compound $BaAg_8S_5$ has been synthesized and analyzed. The computed band structure suggested that it should be a semiconductor. Further study on the transport properties of the title compound will be carried out in the future once large enough crystals can be grown.

ACKNOWLEDGMENTS

We thank Robert L. Bailey of the Department of Geology at Northern Illinois University for the assistance of the microprobe measurement. We also thank the National Science Foundation for the support of our research through Grant DMR-9704048.

REFERENCES

1. R. Xu, A. Husmann, T. F. Rosenbaum, M.-L. Saboungi, J. E. Enderby, and P. B. Littlewood, *Nature* **390,** 57 (1997).
2. R. J. Cava, F. Reidinger, and B. J. Wuensch, *J. Solid State Chem.* **31,** 69 (1980).
3. P. Wu and J. A. Ibers, *Z. Kristallogr.* **208,** 35 (1993).
4. P. Wu and J. A. Ibers, *J. Solid State Chem.* **110,** 156 (1994).
5. P. Wu, M. A. Pell, J. A. Cody, and J. A. Ibers, *J. Alloys Compd.* **224,** 199 (1995).
6. C. L. Teske, *Z. Naturf. B* **34,** 544 (1979).
7. W. Bronger, B. Lenders, and J. Huster, *Z. Anorg. Allg. Chem.* **623,** 1357 (1997).
8. O. J. Guentert and A. Faessler, *Z. Kristallogr.* **107,** 357 (1956).
9. H. G. von Schnering and N. K. Goh, *Naturwissenschaften* **61,** 272 (1974).
10. S. Yamaoka, J. T. Lemley, J. M. Jenks, and H. Steinfink, *Inorg. Chem.* **14,** 129 (1975).
11. G. M. Sheldrick, "SHELXL, Version 5," Siemens Analytical Instruments Inc., Madison, Wisconsin, 1994.
12. A. Altomare, G. Cascarano, C. Giacovazzo, A. Guagliardi, M. C. Burla, G. Polidori, and M. Camalli, *J. Appl. Crystallogr.* **27,** 435 (1994).
13. Y. LePage, *J. Appl. Crystallogr.* **20,** 264 (1987).
14. A. L. Spek, *Acta Crystallogr., Sect. A* **46,** C34 (1990).
15. M. Jasen, *Angew. Chem. Int. Ed. Engl.* **26,** 1098 (1987).
16. R. Hoffmann, *J. Chem. Phys.* **39,** 1397 (1963).
17. M.-H. Whangbo, R. Hoffmann, and R. B. Woodward, *Proc. R. Soc. London A* **366,** 23 (1979).
18. S. D. Wijeyesekera and R. Hoffmann, *Organometallics* **3,** 949 (1984).
19. C. Zheng, *J. Am. Chem. Soc.* **115,** 1047 (1993).
20. M. C. Zonnevylle, R. Hoffmann, P. J. Van Den Hoek, and R. A. Van Santen, *Surf. Sci.* **223,** 233 (1989).
21. M. M. L. Chen and R. Hoffmann, *J. Am. Chem. Soc.* **98,** 1647 (1976).